https://doi.org/10.5194/npg-2021-30
Preprint. Discussion started: 13 September 2021

Nonlinear Processes in Geophysics
Discussions
Open Access
EGU

Estimate of energy loss from internal solitary waves breaking on slopes

Kateryna Terletska[1], Vladimir Maderich[1], and Tatiana Talipova[2]

[1]Institute of Mathematical Machine and System Problems, Glushkov av., 42, Kyiv 03187, Ukraine
[2]Institute of Applied Physics RAS, Nizhny Novgorod,Russian Federation

Correspondence to: Terletska K. (kterletska@gmail.com)

Abstract.

Internal solitary waves (ISW) emerge in the ocean and seas in different forms and break on the shelf zones in a variety of ways. Their breaking on slopes can produce intensive mixing that produces such process as biological productivity and sediment transport. Mechanisms of ISW of depression interaction with the slopes related to breaking and changing polarity as they shoal. We assume that parameters that described the process of interaction of ISW in a two-layer fluid with the idealised shelf-slope are: the non-dimensional wave amplitude α (wave amplitude normalized on the upper layer thickness), the ratio of the height of the bottom layer on the shelf to the incident wave amplitude β and angle γ. Based on three-dimensional $\alpha\beta\gamma$ classification diagram with four types of interaction with the slopes it was discussed: (1) ISW propagates over slope without changing polarity and wave breaking; (2) ISW changes polarity over slope without breaking;(3) ISW breaks over slope without changing polarity; (4) ISW both breaks and change polarity over the slope. Relations between the parameters α,β,γ for each regime were obtained using the empirical condition for wave breaking and weakly nonlinear theory for the criterion of changing the polarity of the wave. In the present paper the α,β,γ diagram was validated for idealised real scale topography configurations. Results of the numerical experiments that were carried out in the present paper and results of field and laboratory experiments from other papers are in good agreement with proposed classification and estimations. Based on 85 numerical experiments ISWs energy loss during interaction with slope topography with $0.5^o < \gamma < 90^o$ was estimated. "Hot spots" zones of high levels of energy loss were shown for idealized configuration that mimics continental shelf at Lufeng Region SCS.

Keywords. Internal solitary waves of depression, wave shoaling, energy loss

1 Introduction

One of the mechanisms of generation of the internal solitary waves (ISWs) in the seas and oceans is the tidal flows over ridges and steep topography, where they transform quickly into internal solitary waves during their propagation. The first mode internal solitary waves are most energetic and usually such waves propagating as waves of depressions when the upper layer thickness is much less than the depth of the ocean. Generated by tides ISWs of depression can propagate thousands of kilometers from the origin (Kunze (2012)). As the result ISWs transport the energy far from the place of their generation. Like surface

https://doi.org/10.5194/npg-2021-30
Preprint. Discussion started: 13 September 2021


Nonlinear Processes in Geophysics
Discussions
Open Access
EGU

waves, internal waves break in the coastal zone of the ocean. Such waves are an important components of mixing and energy dissipation (Liu (1998), Davis (2020)). Depending on the characteristics of the traveling ISW, ocean stratification and characteristics of the continental slope wave on the shelf could be shoaling in different forms. ISW often reach extreme amplitudes, for example in the South China Sea (SCS) (Klymak (2006)). They are well-known contributors to material transport, nutrient supply (Wang (2007)). ISWs in SCS are generated by the interaction of internal tides and the system of two quasi-parallel ridges in the Luzon Strait (Alford (2015)). Such waves could propagate at vast distances toward Dongsha Atoll mainly in the form of mode-1 internal solitary waves where they shoal and dissipate at the shallow continental shelf (Liu (1998)).

During wave shoaling two mechanisms were expected to be essential: (i) wave breaking resulting in mixing and (ii) changing of the polarity of the initial wave of depression over the slope into a wave of elevation on the shallow zone. The conversion of the internal wave of depression into elevation waves in a two-layer stratification is expected if the thickness of the mixed layer is greater than one-half the total water depth (Helfrich (1986),Cheng (2011)). Different types of the breaking locations are commonly distinguished by slope inclination, water column stratification, and wave characteristics (Vlasenko (2002), Aghsaee (2010), Boegman (2005)). A simple three-dimensional $\alpha\beta\gamma$ classification diagram was proposed by (Terletska (2020)) to distinguish different regimes of transformation of ISW over the shelf-slope topography. It is based on three parameters: the slope angle γ, the non-dimensional wave amplitude α (wave amplitude normalized on the upper layer thickness), and the blocking parameter β that is the ratio of the height of the bottom layer on the shelf to the incident wave amplitude.

The present study focused on ISWs transformation over idealised shelf-slope topography with a two-layer stratification. The objectives are to: (1) compare $\alpha\beta\gamma$ classification with the results of numerical modelling, laboratory studies , and field observations, (2) find high energy dissipation zones of ISWs passed over the shelf-slope topography based on regimes classification that includes such parameters as wave amplitude, stratification and slope, (3) for $\alpha\beta\gamma$ classification carry out numerical modeling for idealized configuration that mimics continental shelf at Lufeng Region SCS, (4) determine energy loss of the transformation of ISWs with the shelf-slope topography.

Information about polarity change criteria and criteria of breaking in $\alpha\beta\gamma$ classification of regimes of ISWs transformation over shelf topography is presented in the corresponding Section. The overview of field and laboratory measurement data and their comparison with numerical modelling data are in Section "Data and methods". Dissipation of energy of ISWs breaking over shelf topography discussed in Section "Estimate of energy loss in internal waves breaking on slopes". The results are summarized in the Conclusions.

2 Regimes of ISW transformation over slope-shelf topography

The two-layer approximation is a simple model of the stably stratified oceans and lakes. In this model we approximated stratification by the two continuous layers of depths h_1 (upper layer) and h_2 (lower layer) with relatively thin pycnocline. In the case when $h_1 > h_2$ internal solitary waves propagate in the form of elevation ISW, and if $h_1 < h_2$ in the form of the waves of depression. In this study we will consider ISW of depression (with amplitude a_{in}) propagating over an idealized slope-shelf

https://doi.org/10.5194/npg-2021-30
Preprint. Discussion started: 13 September 2021

Nonlinear Processes in Geophysics
Discussions
Open Access
EGU

with a slope γ and the minimum depth of the lower layer over the shelf h_{2+}. Idealised shelf-slope topography is shown in Fig. 1 b, and the idealised configuration that mimics continental shelf at Lufeng Region (Fig. 1 a) SCS is shown in Fig. 1 c .

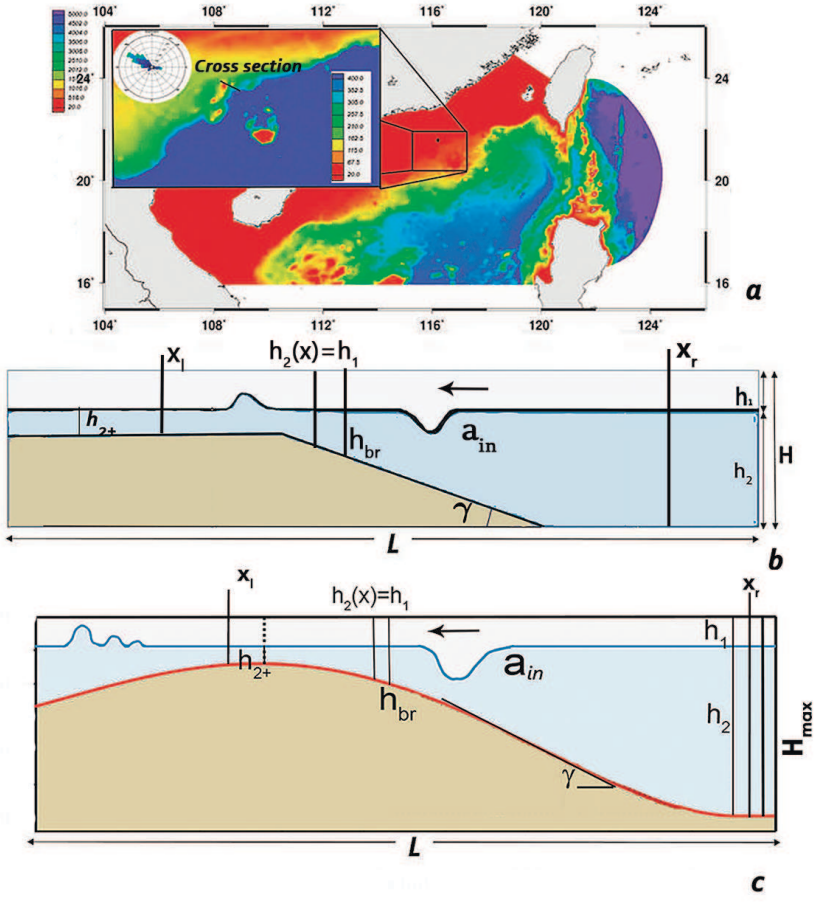

Figure 1. Sketch of transformation of depression ISW over a slope-shelf. (a) - Idealised topography at Lufeng Region (SCS), (b) sketch of breaking and changing the polarity of ISW of depression after passing through a turning point.

It could be assumed that transformation on a slope is controlled by stratification, slope inclination and amplitudes (wavelength) of the incident wave (Terletska (2020)). They determine two possibilities that could occur with the wave during shoaling: (i) ISW breaking, that is associated with gravitational instability due to shear instability and wave overturning and (ii) depression type ISW changing the polarity on the slope. There are different breakers behaviour of ISW in a two-layer fluid over slope were classified by (Aghsaee (2010), Boegman (2005)) into four types: surging, plunging, collapsing, and fission. Classification is based on the ratio of the wave slope and the bottom slope, and was modified for collapsing and plunging breakers with the use of new wave Reynolds number that taking into account nonlinear wave steepening [Nakayama (2019)].

https://doi.org/10.5194/npg-2021-30
Preprint. Discussion started: 13 September 2021


Nonlinear Processes in Geophysics Discussions
Open Access
EGU

According the (Terletska (2020)) three parameters α β γ can be important for behaviour of the incident wave on slope-shelf (fig. 1 b,c):

1. slope inclination γ (measured as an angle);

2. blocking parameter β is the ratio of the height of the minimum depth of the lower layer over the shelf h_{2+} (Fig. 1 b,c) to the incident wave amplitude a_{in}

$$\beta = h_{2+}/|a_{in}|. \tag{1}$$

This idea comes from numerical and laboratory experiments as the "degree of blocking" that is an important parameter that controls the loss of energy into transmitted and reflected waves passing the obstacle (Vlasenko (2002), Wessels (1996)). Parameter B was modified in (Talipova (2013)) where considered ISWs (as depression and elevation type) passing over underwater step $\gamma = 90^o$. It was shown that for the case of ISW of depression for values $\beta > 3$ the ISW transformation over underwater step is weak (when the dynamics of ISW could be described by weakly nonlinear theory), for $2 < \beta < 3$ interaction is moderate (when the main mechanism for ISW breaking over bottom step produce shear instability), for $0.4 < \beta < 2$ interaction is strong with maximal energy loss (when ISW produced the flow that results in a jets and vortices), $-0.9 < \beta < 0.4$ so-called 'transitional regime' (when the step height between strong interaction and full reflection from the step) and for $\beta < -0.9$ full reflection from the underwater step.

3. nonlinearity parameter that is the ratio of the incident wave amplitude to the depth of upper layer:

$$\alpha = |a_{in}|/h_1. \tag{2}$$

Internal waves in a framework of weakly nonlinear theory change their polarity in the point where the upper and lower layers are equal (Grimshaw (2004)). Notice that numerical experiments using full Naiver-Stokes equations (Maderich (2010)) confirm the applicability of the Gardner equation to predict turning point $h_1 = h_2$ even for the wave of large amplitude. This relation for turning point can be expressed through parameters and using

$$\beta = 1/\alpha; \tag{3}$$

For breaking point criteria was taken criterion from Vlasenko (2002). It was build based on the Naiver–Stokes numerical model simulations data. It was found that the ratio of the amplitude of the incident wave a_{in} into the value of the undisturbed thickness of the lower layer in point where the wave breaking takes place h_{br} (Fig. 1 b,c), is the function of the slope γ:

$$\frac{|a_{in}|}{h_{br}} = \frac{0.8^o}{\gamma} + 0.4. \tag{4}$$

https://doi.org/10.5194/npg-2021-30
Preprint. Discussion started: 13 September 2021

Nonlinear Processes in Geophysics
Discussions
Open Access
EGU

For each slope angle γ the blocking parameter value β_{br} that divide zone of non-breaking regime for $\beta > \beta_{br}$ and breaking regime for $\beta < \beta_{br}$ can be found from (3) and (4) at $h_{2+} = h_{br}$ that

$$\beta_{br} = \gamma/(0.8^o + 0.4\gamma). \tag{5}$$

We can also obtain value α_{br} that divide zone 4 on breaking regime when ISW first breaks $\alpha > \alpha_{br}$ and when wave first change polarity and then breaks $\alpha < \alpha_{br}$. It can be found from(3) using (5) that yields

$$\alpha_{br} = (0.8^o + 0.4\gamma)/\gamma. \tag{6}$$

Thus four different scenarios of internal solitary wave interaction of with a shelf-slope topography in a two layer approximation can be realized: (1) breaking regime over the slope-shelf; (2) non-breaking regime over the slope-shelf, (3) polarity change regime and (4) regime of non-polarity change.

Analysing equations (3) (5) we conclude that parameters α, β, γ control the processes as the wave breaking as the wave polarity change. A three-dimensional diagram with the dependence on parameters α, β, γ ($\alpha\beta\gamma$ diagram) is introduced in Fig. 2 with four zones: (zone 1) ISWs transform without changing polarity and wave breaking; (zone 2) ISWs transform with changing polarity without breaking; (zone 3) ISWs break without changing polarity; (zone 4) ISWs break with changing polarity. In the space of α, β, γ these regimes are separated by the surfaces (3)and (5).

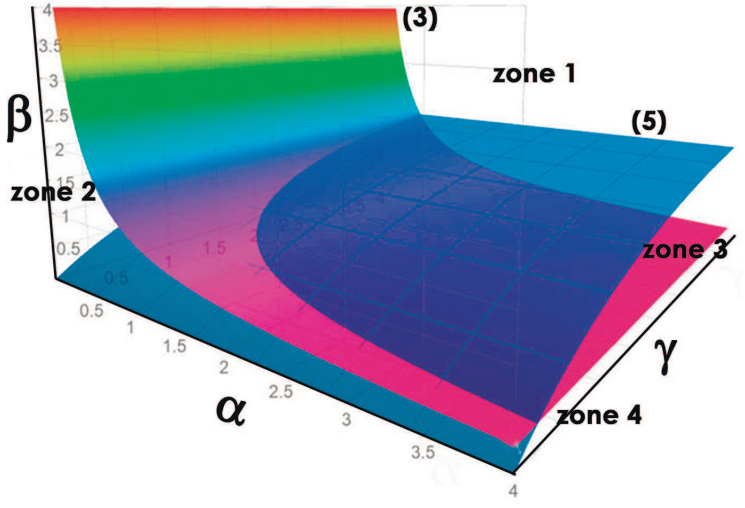

Figure 2. 3D α, β, γ diagram of regimes (zone 1) without changing polarity and wave breaking, (zone 2) - changing polarity without breaking, (zone 3) regime of wave breaking without changing polarity, (zone 4) - breaking with changing polarity.

To compare $\alpha\beta\gamma$ diagram versus the data from field observations, the results of laboratory measurements and numerical simulations were analysed by (Terletska (2020)) for different slopes $\gamma = 1^o, 1.5^o, 3, 14^o, 60^o, 90^o$.

https://doi.org/10.5194/npg-2021-30
Preprint. Discussion started: 13 September 2021

Nonlinear Processes in Geophysics
Discussions
Open Access
EGU

Table 1. Parameters of ISW in numerical experiments for idealised Lufeng Region in SCS

$\lvert a_{in}\rvert$(m)	α	β	γ
20	0.4	1	$1^\circ, 3^\circ, 5^\circ$
50	1	0.4	$1^\circ, 3^\circ, 5^\circ$
100	2	0.2	$1^\circ, 3^\circ, 5^\circ$

In (Terletska (2020)) was shown that results of field observations (Moum (2003), Osborn (1980), Orr (2003), Nam (2010), Fu (2016)), laboratory experiments (Helfrich (1986), Cheng (2011)) and numerical experiments that simulate ISW transformation in laboratory scales (Talipova (2013), Terletska (2020)) are in good agreement with proposed classification. All data were identified as belonged to corresponding diagram domain.

3 Data and methods

Let us consider the transformation of the ISWs in the case of idealised topography and stratification that approximately follows cross section in Lufeng Region in SCS. Position of the cross section is shown in Fig. 1 a. Data indicates (Ramp (2010)) that internal waves from Luzon strait propagate westward to Dongsha Islands and further to Lufeng Region and the measured current in waves is about $1.5 - 2.0$ m/s. Wave amplitudes obtained using SAR images (during May after strong thermocline developing in April) on the depth about 300 m vary from 10 to 50 m with the depth of thermocline about $40 - 65$ m (Junmin (2003)). For numerical modeling of the idealised case that mimics Lufeng Region computational domain with the length $L = 18$ km, and maximal depth $H_{max} = 300$ m was considered (Fig. 1 a). We approximated stratification in the Lufeng Region by the two-layer density profile. The densities of the layers are ρ_1 and ρ_2 (depths h_1 and h_2 and $H = h_1 + h_2$.) and the pycnocline layer thickness dh :

$$\rho(z) = \frac{\rho_1 + \rho_2}{2} - \frac{\rho_1 - \rho_2}{2} \tanh\left(\frac{z - h_1}{dh}\right), \tag{7}$$

In numerical experiments we vary waves amplitudes $|a_{in}|$: $|a_{in}| = 20$ m, $|a_{in}| = 50$ m $|a_{in}| = 100$ and slopes γ: $\gamma = 1^o$, $\gamma = 3^o$, $\gamma = 5^o$. Slope inclination γ for smooth curvilinear slope is measured as the maximal slope value. Corresponding values of α,β,γ are given in the table 1. Density $\rho_1 = 1021.5$ and $\rho_2 = 1025.5$ (kg/m^3) and the pycnocline layer thickness $dh = 15$ m. Density profile from measurements from SCS (May) (Orr (2003)) and initial density profile (7) are shown in Fig. 3. Depths layers are $h_1 = 50$ m and $h_2 = 250$ m for all runs.

The numerical simulations were carried out using the free-surface non-hydrostatic numerical model Kanarska (2003),Maderich (2012) as a nonhydrostatic extension of the Princeton Ocean Model (POM). The Smagorinsky model extended for the stratified fluid (Siegel (1994)) was used to explicitly describe the small-scale turbulent mixing and dissipation effects in the ocean scale NISW. Totaly 9 (three γ and three α) runs with resolution of the computational domain 42002504 were carried out for

https://doi.org/10.5194/npg-2021-30
Preprint. Discussion started: 13 September 2021

Nonlinear Processes in Geophysics
Discussions
Open Access
EGU

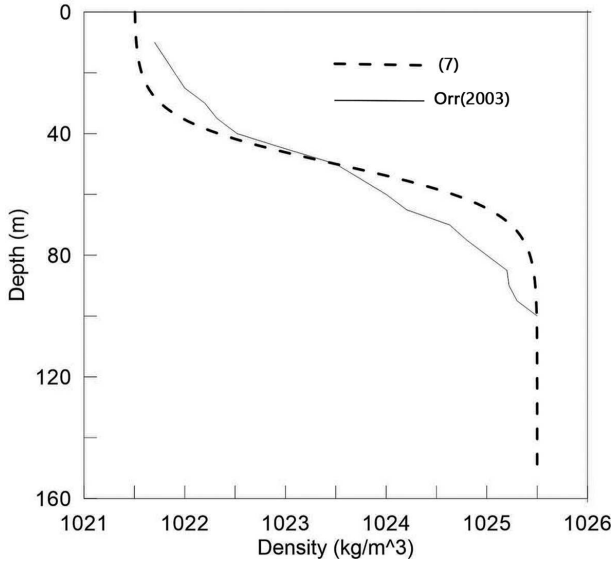

Figure 3. Density profile from measurements from SCS (May) (Orr (2003)) and initial density profile (7) used for numerical calculations

all cases. Spatial resolution was $4.31.21.2$ m for all cases. Bottom following, sigma coordinate vertical system was used in present modeling. The quasi-two-dimensional model with a resolution of 4 nodes across the wave tank was used for present calculations. No-slip boundary conditions were applied at the bottom and two end walls. The free-slip conditions were applied at the side walls. Mode-splitting technique and decomposition of pressure and velocity fields on hydrostatic and nonhydrostatic components were used in numerical method and it is described in detail in (Maderich (2012)).

The model was initialized using iterative solution the Dubreil-Jacotin-Long (DJL) (Dubreil-Jacotin (1932)) equation with the initial guess obtained from a weakly nonlinear theory. The DJLES spectral solver from the MATLAB package https://github.com/mdunphy/DJLES/ was used. In Fig. 4 is shown transformation of ISW with initial amplitude $|a_{in}| = 50$ m. The minimum depth of the lower layer over the shelf is $h_{2+} = 20$ m and the slope is $\gamma = 1^o$. The parameters are $\alpha = 1$, $\beta = 0.4$,$\gamma = 1^o$, that corresponds to regime of breaking with changing polarity. ISWs propagation velocity is about 1.2 m/s that is typical for Lufeng Region in SCS (Junmin (2003)). From (3) and (4) we could found the location on the slope where ISW will change polarity $h_{2+} = h_1 = 50$ m and ISW breaking at the place where $h_{br} \approx 40$ m. It could be seen from Fig. 4 that ISW $|a_{in}| = 50$ m at first changes its polarity at time $t = 2$ h 30 min and then breaks at the slope at $t = 2$ h 40 min.

In Fig. 5 a 3D diagram of regimes with the cross section $\alpha\beta$ for $\gamma = 1^o$ is shown. In the Fig. 5 b red line corresponds to the polarity change criterion (3) whereas the black line corresponds to the breaking criterion (5). Three experiments exp.1: $\alpha = 0.4, \beta = 1, \gamma = 1^o$; exp.2: $\alpha = 1, \beta = 0.4, \gamma = 1^o$; exp.3.: $\alpha = 2, \beta = 0.2, \gamma = 1^o$ are marked. The first one exp.1 represents the cases of interaction of ISW ($|a_{in}| = 50$ m) with polarity change but without breaking. Exp.2 represents the case when first ISW changes its polarity from depression to elevation types and then breaks 4. Exp.3 is the case when ISW brakes on the slope before it pass the changing polarity point.

https://doi.org/10.5194/npg-2021-30
Preprint. Discussion started: 13 September 2021

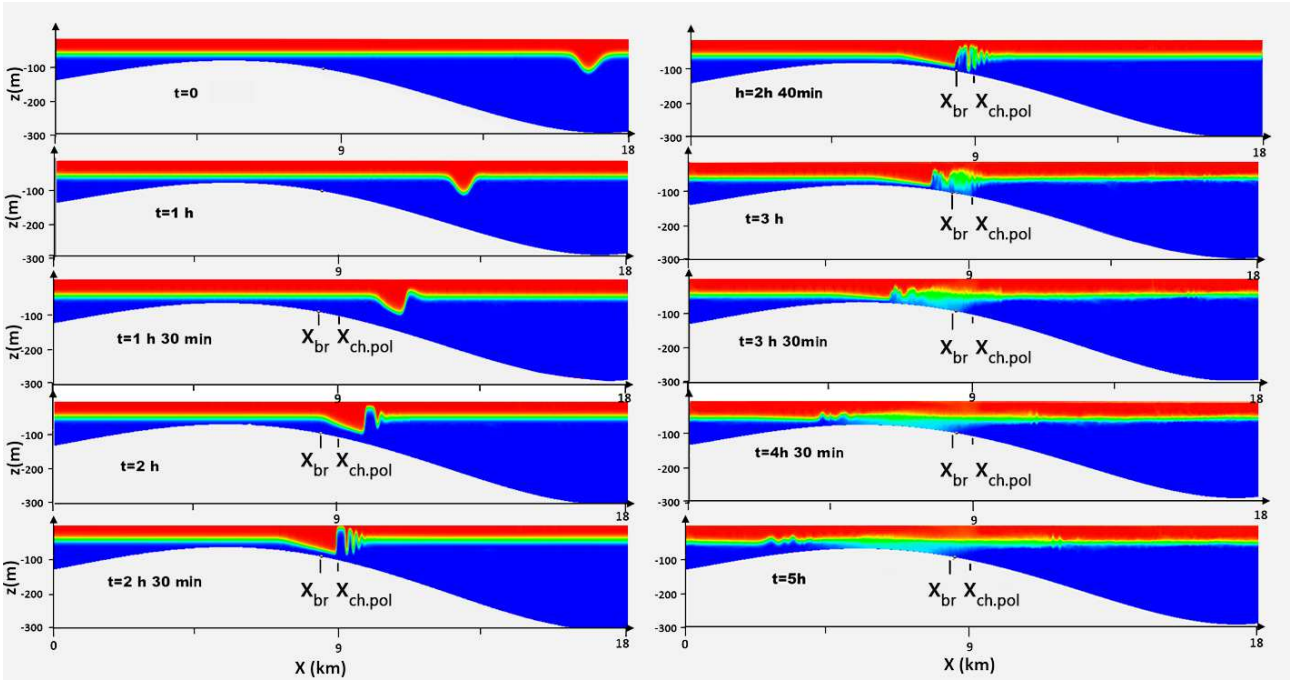

Figure 4. The evolution of the ISW with $|a_{in}| = 50$ m in cross-sections at time $t = 0; 60; 90; 120; 150; 160; 180; 210; 270; 300$s ($\gamma = 1^o$, $\alpha = 1$, $\beta = 0.4$). x_{br} and $x_{ch.pol}$ - are the points of breaking and changing polarity.

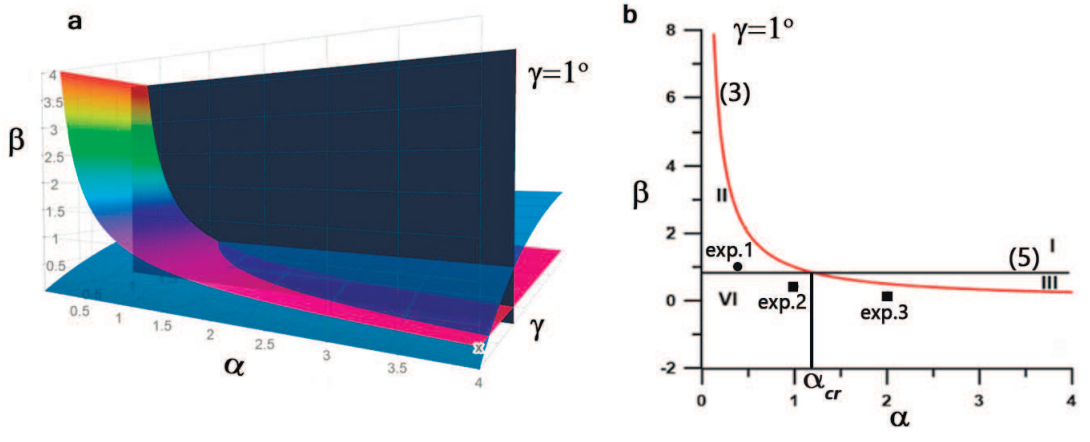

Figure 5. 3D diagram of regimes with the cross-section $\alpha\beta$ for $\gamma = 1^o$. The red line corresponds to polarity change criterion (3), black line corresponds to breaking criterion (5). The circles are changing polarity without breaking cases, squares mark cases of changing polarity with breaking.

https://doi.org/10.5194/npg-2021-30
Preprint. Discussion started: 13 September 2021

Nonlinear Processes in Geophysics
Discussions
Open Access
EGU

Table 2. Parameters of ISW in numerical experiments of laboratory scale [Terletska (2020)].

$\lvert a_{in}\rvert$(m)	α	β	γ
0.02	0.25	$0, 1, 2.5$	$0.5^o, 1.5°, 60°, 90°$
0.08	1	$0.3, 1.1, 2.2$	$0.5^o, 1.5°, 60°, 90°$
0.15	1.5	$0, 1.5, 2.5$	$0.5^o, 1.5°, 60°, 90°$
0.15	1.5	$0.58, 0.8, 1.41$	$1.5°$

4 Estimate of energy loss in internal waves breaking on slopes

An important characteristic of the wave-slope interaction is the loss of kinetic and available potential energy during the transformation. Energy transformation due to mixing leads to the transition energy to background potential energy and to the energy dissipation. It can be estimated based on the budget of the wave energy before and after the transformation.

It was carried out calculating of energy dissipation for two configurations - for real scale experiment for idealised Lufeng Region in SCS and laboratory scale experiment with the trapezoid shelf-slope configurations (Terletska (2020)). Parameters of ISW in numerical experiments of laboratory scale experiments (from (Terletska (2020)) are given in table 2.

The characteristics of the incoming and reflected wave were recorded in the cross-sections x_r, which are located near the foot of the slope, and the wave passing on the shelf, in the cross-section x_l (Fig. 1 b,c). The sum of kinetic and available potential that is the pseudoenergy energy was calculated by integration in time of the energy fluxes of these waves at the sections x_l (of transmitted waves) x_r (of incident and reflected waves). The detailed method of estimation of available potential energy was discussed in (Talipova (2013)). The relative estimation of the energy loss δE_{loss} is given by

$$\delta E_{loss} = (PSE_{in} - PSE_{tr} - PSE_{ref})/PSE_{in}. \tag{8}$$

where PSE_{in} - is pseudoenergy of incident wave, PSE_{tr} and PSE_{ref} - is pseudoenergy of transmitted and incident ones respectively. The energy loss for mixing during the interaction of the wave with the slope of $\delta E_{loss}(\%)$ from the blocking parameter β is shown in fig. 6 a. This field of values $\gamma\beta$ is built by 39 numerical experiments described in table 2, 37 numerical experiments from (Talipova (2013)) for $\gamma = 90^o$ and 9 experiments from the present study. δE_{loss} was estimated for the wide the range of slopes $0.5^o < \gamma < 90^o$ and blocking parameters $-2 < \beta < 8$. ISW energy loss for limiting case of underwater step when $\gamma = 90^o$ was compared with the results of laboratory experiments (Wessels (1996)) and (Chen (2007)) 6 b. It can be seen that interaction in zone 4 is the most dissipative. With this type of interaction, energy losses reach up to 55%. For slopes from $5^o < \gamma < 90^o$ dependence of the energy dissipation from the blocking parameter β has almost the same pick shape as in the limiting case $\gamma = 90^o$. For mild slopes γ we will expect increase of dissipation for all range of blocking parameter values β.

We can compare the energy dissipation for real scale experiment with the laboratory scale experiment with a close values of α and β for slope $\gamma \approx 1$. Consider the cases with $\alpha = 1$ and $\beta = 0.4$ for slope $\gamma = 1°$ (real scale from table 1) and $\alpha = 1$ and

https://doi.org/10.5194/npg-2021-30
Preprint. Discussion started: 13 September 2021

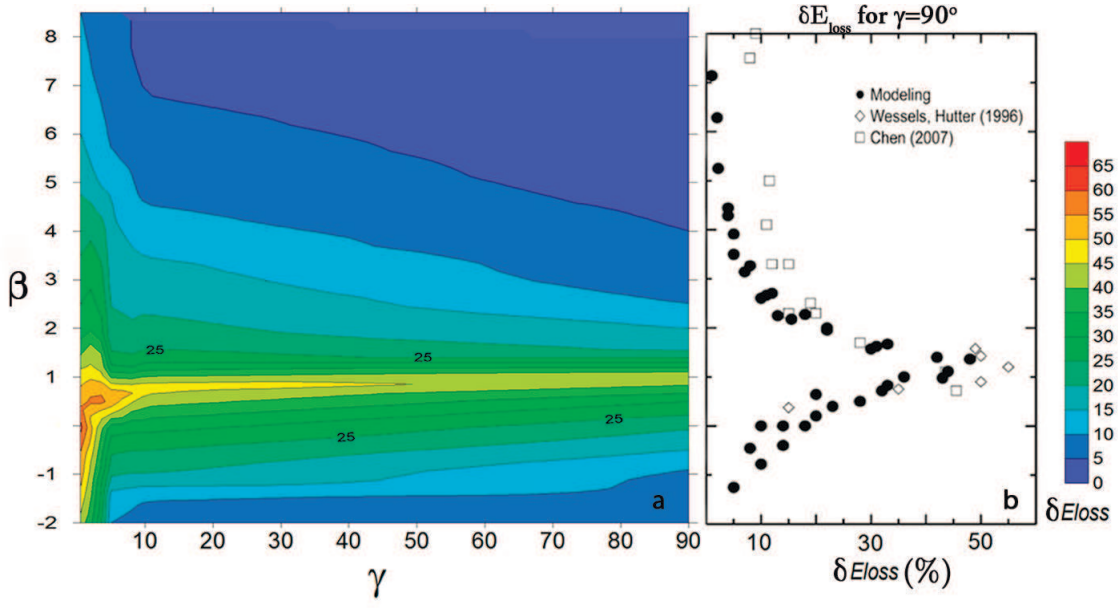

Figure 6. Energy loss δE_{loss} in internal waves breaking on slopes for γ from 0.5° to 90°. For limiting case $\gamma = 90^\circ$ it corresponds to the numerical experiments Talipova (2013) and the results of laboratory experiments Wessels (1996) and Chen (2007) with steep obstacles.

$\beta = 0.3$ for slope $\gamma = 1.5^\circ$ (laboratory scale experiments table 2) (zone 4 - wave breaking regime with polarity change). For strong mixing the difference is about 5% $\delta E_{loss_{r_s}}$ =62 %, $\delta E_{loss_{l_s}}$=57 %.

To build a zone map for the shelf zone the direction of propagation of internal waves is necessary. It could be found using approach for estimating the geographic location of high-frequency nonlinear internal waves from (Jackson (2012)), amplitudes of the incoming internal waves, the depth of the mixed layer. Fig. 7 shows an example of a map with zones corresponding to the different regimes of interaction described above. These maps were constructed for the case of internal waves with an amplitude of $a_{in} = 50$ m and a mixed layer depth h_1 = 50 (Junmin (2003)). On this map the black line - is isobath 120 m (shelf), the violet line is polarity change curve $h_1 = h_2$ and the red area - is the zone of internal wave breaking where $h_1 + h_{br} > H$.

5 Conclusions

A three-dimensional $\alpha\beta\gamma$ classification diagram with four types of interaction of ISWs with the slopes was discussed. Relations between the parameters α, β, γ for each regime were obtained using the empirical condition for wave breaking and weakly nonlinear theory for the criterion of changing the polarity of the wave. The regimes are: (1) ISW propagates over slope without changing polarity and wave breaking; (2) ISW changes polarity over slope without breaking;(3) ISW breaks over slope but without changing polarity; (4) ISW both breaks and change polarity over a slope. The diagram was validated for realistic topography configurations. Numerical modeling of the idealized configuration that mimics the continental shelf at Lufeng

https://doi.org/10.5194/npg-2021-30
Preprint. Discussion started: 13 September 2021

Nonlinear Processes in Geophysics
Discussions
Open Access
EGU

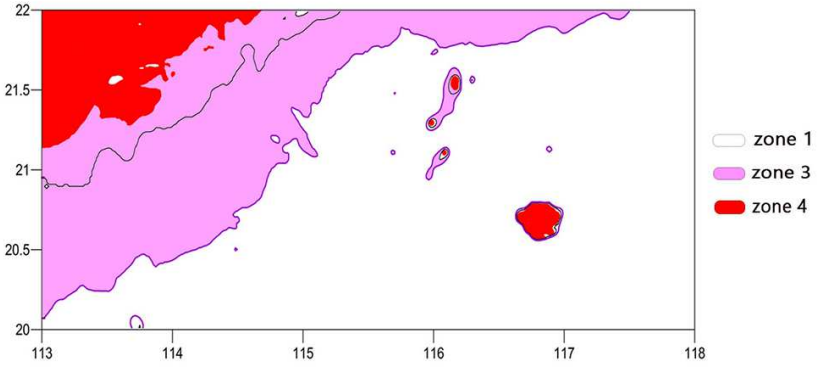

Figure 7. Zone map for internal waves transformation over South China Sea shelf with an initial amplitude of 50 m and a depth of the mixed layer 50 m.

Region SCS was carried out. Results numerical experiments that were carried out in the present paper and other laboratory experiments are in good agreement with the proposed classification and estimations. Based on present numerical experiments internal solitary loss of wave energy from interaction with the slope topography was estimated. We concluded that the results of field, laboratory, and numerical experiments are in good agreement with the proposed classification which can be used for identification of 'hot spots' of energy dissipation in the ocean.

Code and data availability. The output files for all numerical experiments reported in the paper are available from the corresponding author.

Author contributions. KT and VM conceived the idea, KT carried out numerical simulations, contributed to the design of figures and participated in the writing of the manuscript. TT commented on writing of the manuscript contributed large parts of the manuscript organization and interpretation of the results. VM contributed to writing the manuscript and interpretation of the results.

Competing interests. The authors declare that they have no conflict of interest.

Acknowledgements. This work was partially supported Russian Foundation of Basic Research (grant No 19-05-00161) (TT)

https://doi.org/10.5194/npg-2021-30
Preprint. Discussion started: 13 September 2021

References

Kunze, E., MacKay, C., McPhee-Shaw, E. E., Morrice, K., Girton, J. B., and Terker, S. R.: Turbulent mixing and exchange with interior waters on sloping boundaries, The Journal of Physical Oceanography, 42, 910–927 ,doi: 10.1175/JPO-D-11-075.1, 2012.

Liu, A. K., Chang, S. Y., Hsu, M.-K. and Liang, N. K.: Evolution of nonlinear internal waves in the East and South China Seas, Journal of Geophysical Research, 103, 7995-8008, 1998.

Davis, K. A., Arthur, R. S., Reid, E.C., Rogers, J. S., Fringer, O. B. , DeCarlo, T. M., Cohen, A.L.: Fate of Internal Waves on a Shallow Shelf, Journal of Geophysical Research, 521, 65-69, 2020.

Klymak, J.M., Pinkel, R., Liu, C.T., Liu, A.K., David, L.: Prototypical solitons in the South China Sea, Geophysical Research Letters , 33 , L11607, doi:10.1029/ 2006GL025932,2006.

Wang, Y. H., Dai, C. F., Chen, Y. Y.: Physical and ecological processes of internal waves on an isolated reef ecosystem in the South China Sea, Geophysical Research Letters, 34, 1–7, 2007.

Alford, M.N., Peacok, T., Mackinnon, J.A. Tang, D.: The formation and fate of internal waves in the South China Sea, Nature, 521,65-69,2015.

Helfrich, K. R., Melville, W. K.: On long nonlinear internal waves over slope-shelf topography, Journal of Fluid Mechanics, 167, 285-308, 1986.

Chen, C.-Y.: An experimental study of stratified mixing caused by internal solitary waves in a two-layered fluid system over variable seabed topography, Ocean Engineering, 34 1995–2008,2007.

Vlasenko, V.I., Hutter, K.: Numerical experiments on the breaking of solitary internal waves over a slope shelf topography. The Journal of Physical Oceanography, 32, 1779-1793, 2002.

Aghsaee, P., Boegman, L., Lamb, K.G.: Breaking of shoaling internal solitary waves, Journal of Fluid Mechanics, 659, 289–317, https://doi.org/10.1017/S002211201000248X,2010.

Boegman, L. Ivey G. N., Imberger, J.: The degeneration of internal waves in lakes with sloping topography, Limnology and Oceanography, 50 , 1620–1637, https://doi.org/10.4319/lo.2005.50.5.1620,2005.

Terletska, K., Choi, B. H., Maderich, V., and Talipova, T.: Classification of internal waves shoaling over slope-shelf topography, Russial Journal of Earth Scienses, 20, doi:10.2205/2020ES000730, 2020.

Nakayama, K., Sato, T, Shimizu, K., and Boegman, L.: Classification of internal solitary wave breaking over a slope, Physical Review Fluids, 4, 014801,2019. https://doi.org/10.1103/PhysRevFluids.4.014801

Wessels, F., Hutter, K.: Interaction of internal waves with a topographic sill in a two-layered fluid, Journal of Physical Oceanography , 26(2), 5–20, 1996.

Talipova, T., Terletska, K., Maderich, V., Brovchenko, I., Pelinovsky, E., Jung, K.T., Grimshaw, R.: Solitary wave transformation on the underwater step: Asymptotic theory and numerical experiments, Physics of Fluids, 25 , doi: 10.1063/1.4797455, 2013.

Grimshaw, R., Pelinovsky, E., Talipova, T, Kurkin, A.: Simulation of the transformation of internal solitary wave on oceanic shelves, Journal of Physical Oceanography, 34,2774–2791,2004.

Maderich, V., Talipova, T., Grimshaw, R., Terletska, K., Brovchenko, I., Pelinovsky, E., Choi, B.H.: Interaction of a large amplitude interfacial solitary wave of depression with a bottom step, Physics of Fluids, 22, DOI: 10.1063/1.3455984, 2010.

Moum, J.N., Farmer, D.M., Smyth, W.D., Armi, L., Vagle, S.: Structure and generation of turbulence at interfaces strained by internal solitary waves propagating shoreward over the continental shelf, Journal of Physical Oceanography, 33, 2093-2112, 2003.

https://doi.org/10.5194/npg-2021-30
Preprint. Discussion started: 13 September 2021

Osborn, A., Burch, T., Butman, B., Pineda, J: Internal solitons in the Andaman Sea, Science, 208, 4443,451–460, doi:10.1029/2008JC00472,1980.

Orr, M.H., Mignerey, P.C.: Nonlinear internal waves in the South China Sea: observation of the conversion of depression internal waves to elevation internal waves, J. Geophys. Res, 108(C3), 3064-2010, 2003.

Nam S. H. and Send U.: Direct evidence of deep water intrusions onto the continental shelf via surging internal tides, Journal of Geophysical Research, 116, doi:10.1029/2010JC00669, 2010.

Fu, K.-H., Wang, Y.-H, Lee, C.P., Lee, I. H.: The deformation of shoaling internal waves observed at the Dongsha Atoll in the northern South China Sea, Coastal Engineering Jornal, 58, 1650001, 10.1142/S0578563416500017, 2016.

Ramp, S.R., Yang, Y.-J., Bahr, F.L.: Characterizing the nonlinear internal wave climate in the northeastern South China Sea, Nonlinear Processes in Geophysics, 17(5), DOI:10.5194/npg-17-481-2010, 2010.

Junmin, M.,Zhang, J.: An Experiment of Internal Waves Observation by Synthetic Aperture Radar, Proceedings of ACRS, 1343-1345,2003.

Kanarska, Y., Maderich, V.: A non-hydrostatic numerical model for calculating free-surface stratified flows, Ocean Dynamics, 53, 176-185, 2003.

Siegel, D.A., Domaradzki, J.A.: Large-eddy simulation of decaying stably stratified turbulence, Journal of Physical Oceanography, 24, 2353–2386, 1994.

Maderich, V., Brovchenko, I., Terletska, K., Hutter, K.: Numerical simulations of the nonhydrostatic transformation of basin-scale internal gravity waves and wave-enhanced meromixis in lakes Ch. 4 in Hutter K. (Ed.) Nonlinear internal waves in lakes, Springer. Series: Advances in Geophysical and Environmental Mechanics, 193-276 ,2012.

Dubreil-Jacotin, L.: Sur les ondes type permanent dans les liquides heterogenes, Atti R. Accad. Naz. Lincei, Mem. Cl. Sci.Fis., Mat. Nat, 15, 44-72, 1932.

Cheng, M.H., Hsu, J.R.C.: Effects of varying pycnocline thickness on interfacial wave generation and propagation, Ocean engineering, 88, 34-45, 2014. https://doi.org/10.1016/j.oceaneng.2014.05.018

Cheng, M.H, Hsu, JRC, Chen, C.Y.: Laboratory experiments on waveform inversion of an internal solitary wave over a slope-shelf, Environ Fluid Mech, 11, 353 – 384,2011.

Jackson, C.R., J.C.B. da Silva, and Jeans, G.: The generation of nonlinear internal waves, Oceanography, 25(2), 108–123,2012.